Journal of Applied Polymer Science

Polylactide Stereocomplex Crystallization Prompted by Multiwall Carbon Nanotubes

I. Martínez de Arenaza,[1] Jose R. Sarasua,[1] Hegoi Amestoy,[1] Nerea Lopez-Rodriguez,[1] Ester Zuza,[1] Emilio Meaurio,[1] Franck Meyer,[2] Jose I. Santos,[3] Jean-Marie Raquez,[2] Philippe Dubois[2]

[1]University of the Basque Country (UPV/EHU), Department of Mining-Metallurgy Engineering and Materials Science, Basque Excellence Research Center for Macromolecular Design and Engineering POLYMAT, School of Engineering, Alameda de Urquijo s/n 48013 Bilbao, Spain

[2]Center of Innovation and Research in Materials and Polymers (CIRMAP), University of Mons (UMONS), Place du Parc 20, 7000 Mons, Belgium

[3]General Services of Research SGIKER, University of the Basque Country (UPV/EHU), Edificio Joxe Mari Korta Avda. Tolosa, 72 20018 Donostia-San Sebastian, Spain

Correspondence to: Jose R. Sarasua (E-mail: jr.sarasua@ehu.es)

ABSTRACT: Nanocomposites of equimolar enantiomeric polylactide blends with multiwall carbon nanotubes (MWCNTs) were prepared by a solvent casting/sonication procedure. The first objective of the study was to investigate the effect of MWCNTs as nucleating agents for the selective crystallization of the polylactide (PLA) stereocomplex to obtain PLA-based nanocomposites. Transmission Electron Microscopy (TEM) studies revealed large agglomerates and poor distribution of the non-functionalized MWCNTs within the matrix. To enhance the compatibility between PLA and MWCNTs, pyrene-end-functionalized PLLA (py-end-PLLA) nanocomposites were prepared because of the ability of the pyrene moieties to interact with the MWCNTs via $\pi-\pi$ stacking, and were subsequently blended with poly(D-lactide) (PDLA) to investigate the possibility of achieving nanocomposites in which the enantiomeric blend crystallizes as stereocomplex. The resulting nanocomposites were characterized by Differential Scanning Calorimetry (DSC), X-ray Diffraction (XRD), TEM, and Nuclear Magnetic Resonance Spectroscopy (NMR), revealing that MWCNTs were efficient nucleating agents for the overall crystallization of the blends. Interestingly, full stereocomplexation could be achieved with the aid of soft specific thermal treatments. According to these results, the addition of small amounts of MWCNTs combined with a mild thermal treatment might extend the processing window for the preparation of polylactides exclusively crystallized in the stereocomplex form. © 2013 Wiley Periodicals, Inc. J. Appl. Polym. Sci. 130: 4327–4337, 2013

KEYWORDS: biodegradable; composites; crystallization; differential scanning calorimetry; nanotubes; graphene and fullerenes

Received 17 February 2013; accepted 30 June 2013; Published online 17 July 2013
DOI: 10.1002/app.39721

INTRODUCTION

Polylactides (PLAs) are biodegradable and biocompatible aliphatic polyesters derived from renewable resources, non-toxic for the human body and the environment. PLAs have been used as biomedical materials for tissue regeneration, matrices for drug delivery systems, sutures and scaffolds[1] and as alternatives for commercial polymeric materials to reduce the impact on the environment.[2]

Since stereocomplexation between PLLA and PDLA homopolymers was reported in 1987 by Ikada et al.[3] numerous studies have been devoted to the formation, structure, properties, degradation, and applications of the PLA stereocomplexes.[4–9] The stereocomplex crystals show different properties compared with those of PLLA or PDLA crystals.[10] The stereocomplex shows a melting temperature (T_m) approximately 50°C higher than the T_m of either PLLA or PDLA. This significant increase is due to hydrogen bonding interactions in the stereocomplex crystalline structure.[11,12] Stereocomplex crystallization can be considered one of the most effective and promising method to improve the mechanical and thermal properties[13] and also the hydrolytic degradation resistance[14,15] of PLA-based materials. However, the length of L- and D-lactyl unit sequences is a crucial parameter for the stereocomplexation because the homocrystallization prevails over stereocomplex crystallization when blends are prepared from high molecular weight PLLA and PDLA, as it has been concluded in our previous studies;[10,16,17] yet, high molecular weights are required for most polylactide applications.[18,19]

Applied Polymer SCIENCE

Table I. Characteristics of the Commercial Enantiomeric Polylactides

Materials	RS (%)	RM (%)	α (deg)	$[\eta]$ (dL/g)	M_n (g/mol)	D
PDLA	<0.03	<0.2	+158.2	5.68	3.5×10^5	1.92
PLLA	<0.01	<0.1	−158.3	1.54	1.2×10^5	1.25

Carbon nanotubes (CNTs) are considered of great interest in materials science due to their extraordinary electrical and mechanical properties[20–22] and thermal conductivity,[23] hence CNTs are considered potentially excellent reinforcements to obtain polymeric composites.[24,25] The properties of the composites depend on the dispersion of CNTs within the matrix,[26,27] as well as on the strength of the interaction between the polymer and the CNTs.[28] It is well known that in their pristine state CNTs tend to form agglomerates due to π–π stacking interactions and van der Waals bonds.[29] Therefore, a variety of chemical and physical methods have been used to obtain good dispersions of the CNTs within polymer matrices. The different strategies include chemical modification,[30] covalent attachments of monomers, oligomers, and polymers,[31] adsorption of charged surfactants and polyelectrolytes,[32] wrapping with polymers,[33] non-wrapping adsorption of partially collapsed block copolymers,[34] and complexation by π–π[35,36] or cation–π interactions.[37]

Recently, many researchers have encouraged the investigation of the enhancement of the CNT dispersion using appropriate functional groups that may include aromatic compounds such as pyrene, which is electronically very similar to graphite, to accomplish π–π stacking interactions with the graphitic structure of the CNTs.[38–41] The surface modification of the CNTs by pyrene-containing polymers of different nature and molecular architecture can be a very straightforward and efficient method for making them dispersible in a wide variety of solvents, and for preparing homogenous CNT-based polymer composites.[42,43]

Among other factors, the enhancement of crystallization by CNTs acting as nucleating agent can also be crucial to improve the properties of polylactides. CNTs strongly improve the heterogeneous nucleation of the polymer matrices increasing the nucleation density and thus the overall crystallization rate.[44,45] This phenomenon occurs by molecular interactions between the polymer matrix and the surface of the nucleating agent, causing the reduction of the free energy, necessary to form a stable nucleus.[19] Besides CNTs, both inorganic[46,47] and organic nucleating agents[48–51] have been investigated in the crystallization of polylactides. However, little is known about the effect of these nucleating agents in the selective stereocomplex formation in enantiomeric polylactide blends.

In this article, PDLA/PLLA multiwall carbon nanotube (MWCNT) nanocomposites were analyzed in order to evaluate the nucleating effect of the MWCNTs to form stereocomplex crystals in high molecular weight polylactide enantiomeric equimolar blends. It will be shown that the use of pyrene-end-PLLA as compatibilizer in PDLA/MWCNTs blends improves the dispersion of the MWCNTs and, at the same time, influences positively in the formation of stereocomplex crystals.

EXPERIMENTAL

Materials

Commercial poly(D-lactide) and poly(L-lactide) of high optical purity (100%) and molecular weight were supplied by PURAC BIOCHEM (The Netherlands). Table I summarizes important properties of the as received polylactides, including Residual Solvent (RS), Residual Monomer (RM), rotatory power (α), and intrinsic viscosity ($[\eta]$) in $CHCl_3$ at 25°C. Number-average molecular weights (M_n) and dispersity (D) were determined relative to PS standards by GPC in $CHCl_3$ at 25°C.

Pyrene-end-functionalized PLLA (py-end-PLLA) of different molecular weights (2900, 9000, and 24,900 g/mol) were synthesized following the method described in the following section.

MWCNTs (Graphistrenght™ C100) were provided by Arkema (France). A pristine MWCNT is featured by a length in the range 0.1–10 μm, an outer mean diameter in the range 10–15 nm and a mean number of walls ranging from 5 to 15. The degree of purity is around 90%.

Synthesis of Poly(L-lactide) (PLLA) and Pyrene-End-Functionalized PLLA (py-end-PLLA)

Py-end-PLLA was synthesized in chloroform solution (20 mL) by Ring Opening Polymerization (ROP) of L-lactide (5.8 g, 40.3 mmol) initiated with 1-pyrenemethanol (132 mg, 0.57 mmol) and catalyzed by 1,8-diazobicyclo[5.4.0]undec-7-ene (DBU) (21 μl, 0.15 mmol). After stirring the solution at room temperature for 10 min in presence of the catalyst, three drops of acetic acid were added, and the organic layer was washed two times with HCl (0.1*M*). Finally, the compound was precipitated in *n*-hexane and dried under vacuum overnight at 60°C. The yield obtained was around 90%. Non-functionalized poly(L-lactide), PLLA, was also synthesized to be used as reference. ROP of L-lactide was initiated with isopropanol in presence of DBU as catalyst. The reaction was performed at room temperature using chloroform as solvent. PLLA was washed with HCl 0.1*M*. The organic phase was precipitated in *n*-hexane. After filtering, the solid was dried in a vacuum oven overnight at 40°C under reduced pressure.[36,37] The reaction schemes of the synthesis are shown in Figure 1. Table II displays the molecular weight and thermal properties of the synthesized PLLA and py-end-PLLAs.

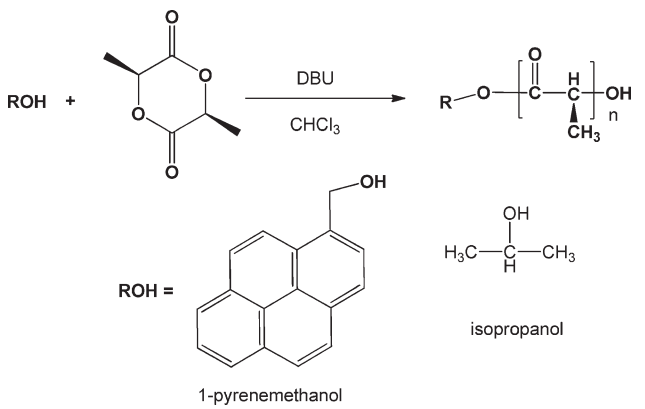

Figure 1. ROP of L-Lactide from 1-pyrenemethanol and isopropanol.

Table II. Molecular Weight and Thermal Properties of the Synthesized Polylactides

Materials	T_m [a] (°C)	ΔH_m [a] (J/g)	M_n [b] (g/mol)	D[b]
py-end-PLLA2900	134.8	60.8	2900	1.17
py-end-PLLA9000	139.0	58.4	9000	1.11
py-end-PLLA24900	142.0	27.4	24900	1.13
PLLA24900	152.9	30.5	24900	-

[a] Determined by DSC analysis in THF at 35°C using universal calibration.
[b] Determined by SEC in THF at 35°C using universal calibration.

Preparation of Enantiomeric Blends

Previous studies have demonstrated that stereocomplexation is favored in blends with equimolar composition.[52,53] In this study, polylactide blends and nanocomposites from equimolar compositions of two enantiomeric polylactides (PDLA and PLLA or py-end-PLLA) were prepared. Py-end-PLLA of different molecular weights (2900, 9000, and 24,900 g/mol) and different amounts of MWCNTs (0.5, 1.0, 1.5, and 3.0 wt %) were used for nanocomposite formulations.

PDLA/PLLA and PDLA/py-end-PLLA blends were prepared by solvent casting. Pellets were dried in vacuum at 100°C for 24 h before preparation of polymer solutions. Solutions of PDLA and PLLA (or py-end-PLLA) were separately prepared by dissolving 125 mg of both polymers in 10 mL chloroform. The two solutions were mixed together with vigorous stirring, followed by solvent evaporation at room temperature for about 3 days.

PDLA/PLLA and PDLA/py-end-PLLA nanocomposites containing 0.5, 1.0, 1.5, and 3.0 wt % of MWCNTs were prepared according to the following procedure. The required amount of nanotubes was first dispersed in chloroform and subjected to tip-sonication during 20 min in an ice bath. Subsequently, the desired composite compositions were prepared by mixing the nanotube dispersions with the PDLA/PLLA or PDLA/py-end-PLLA blend solutions. These mixtures were again sonicated for additional 30 min, and finally allowed to evaporate at room temperature for 48 h.

DSC Analysis

Thermal properties of blends were evaluated using a Differential Scanning Calorimetry (DSC) from TA instruments, model DSC Q200. The DSC was calibrated using the melting temperature and enthalpy of indium. Approximately 5 mg of sample were placed in the aluminium pans for measurement under N_2 atmosphere. A DSC scan from 0°C to 250°C at a heating rate of 10°C/min was used to evaluate the crystallization and melting behavior of samples. Degrees of crystallinity were calculated according to the equations used in previous articles using the values of $\Delta H^0_m = 106$ J/g for PLA homocrystals and $\Delta H^0_m = 142$ J/g for stereocomplex crystallites.[10,16]

X-ray Diffraction (XRD)

The X-ray powder diffraction patterns were collected by using a PHILIPS X'PERT PRO automatic diffractometer in theta-theta configuration, secondary monochromator with Cu $K\alpha$ radiation ($\lambda = 1.5418$ Å) and a PIXcel solid state detector. The sample was mounted on a zero background silicon wafer fixed in a generic sample holder. Data were collected from 10 to 25° 2θ (step size = 0.026°) at room temperature and at 0°C after cooling at 5°C/min from 250°C.

TEM Analysis

Dispersion of MWCNTs was evaluated by Transmission Electron Microscopy (TEM) with a TECNAI G2 20 TWIN instrument under an acceleration voltage of 200 kV. Ultrathin sections with thickness of around 100–1200 nm were used for TEM observations. Sections were cut under cryogenic conditions (−80°C) using a Leica EM FC6 ultramicrotome.

NMR Analysis

1D ^{13}C NMR spectra were obtained using a Bruker 400 WB Plus spectrometer at room temperature. Spectra were collected by using a 4 mm CP-MAS probe spinning at 10,000 Hz. CPMAS ^{13}C NMR spectra of solid samples were recorded for 24 h using the standard pulse sequence, at 100.6 MHz, a time domain of 2 K (2048 data points), a spectral width of 29 KHz, a contact time of 1.5 ms and an interpulse delay of 5 s.

2D diffusion-ordered (DOSY) NMR experiments were obtained using a standard Bruker protocol with a 400 MHz Avance spectrometer equipped with a broad-band *z*-gradient probe; 32 1D ^1H spectra were collected with a gradient duration of 2 ms and an echo delay of 100 ms for PLLA, or 250 ms for the py-end-PLLA. Acquisition times of about 16 and 32 min were required for the PLLA samples and py-end-PLLA. The ledbpg2s pulse sequence, with stimulated echo, longitudinal eddy current compensation, bipolar gradient pulses, and two spoil gradients, was run with a linear gradient (53.5 Gcm_1) stepped between 2% and 95%. The 1D ^1H spectra were processed and automatically baseline-corrected. The diffusion dimension, zero-filled to 1 k, was exponentially fitted according to pre-set windows for the diffusion dimension.

RESULTS AND DISCUSSION

Stereocomplexation of PDLA/PLLA Blends

Figure 2 shows the thermograms of the two enantiomeric optically pure polylactides (PDLA and PLLA) and their 50/50 blend, prepared by solvent casting. All curves exhibit the typical exotherm corresponding to the cold crystallization and the endotherm corresponding to the melting of crystals. In the case of the 50/50 blend, there is a double endothermic peak, one around 170°C, corresponding to the melting of homocrystals, and a small melting peak at about 230°C, corresponding to the melting of a small amount of stereocomplex crystals.

With the aim of increasing the stereocomplex formation in the 50/50 blends, specific isothermal crystallizations were performed. Table III shows the thermal properties of the 50/50 blend crystallized isothermally at 140, 160, 180, and 190°C for 1 and 24 h. It can be noted that the crystalline amount of polymers depends on thermal treatments carried out on samples. These thermal treatments included melting of the polymer sample at a temperature of 250°C for 2 min, followed by quenching

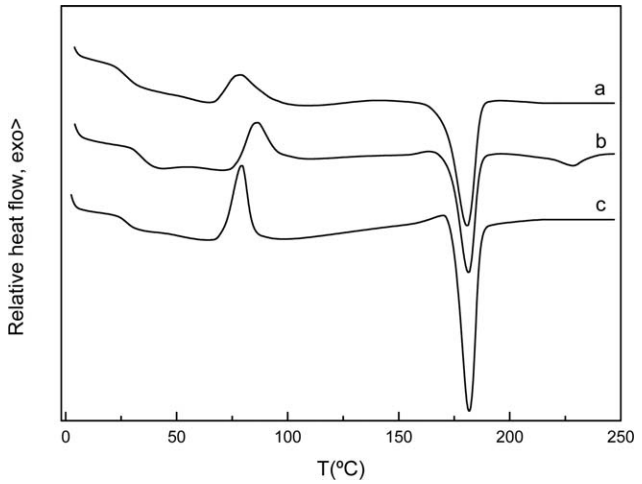

Figure 2. DSC curves of as-cast (a) PDLA, (b) non-functionalized 50/50 blend, (c) and PLLA.

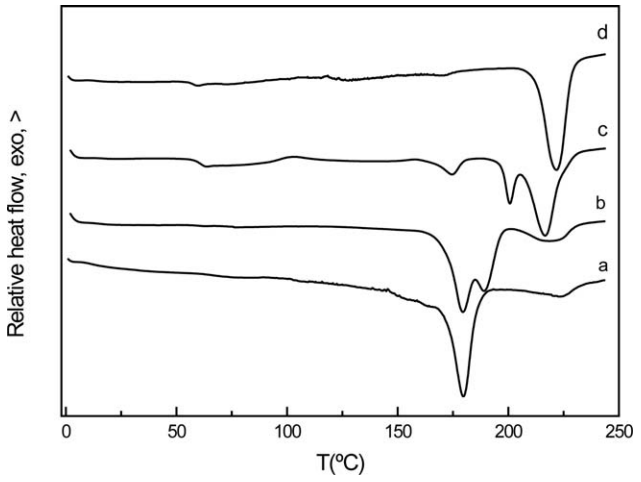

Figure 3. DSC curves of 50/50 blend after annealing for 24 h at (a) 140°C, (b) 160°C, (c) 180°C, and (d) 190°C.

to the selected crystallization temperature comprised between 140 and 190°C.

As can be seen in Table III, in the 50/50 blends annealed for 1 h at temperatures below 180°C, the homocrystal melting enthalpies are larger than the stereocomplex melting enthalpies, indicating that homocrystal formation is favored at these conditions. After annealing 24 h, the overall crystallinity degree of the samples is slightly increased, but the relative amounts of crystalline forms remain almost unchanged. However, when the selected crystallization temperature reaches the melting temperature of the homocrystals (180–190°C), the crystal type formation is drastically reversed. After annealing at 190°C for 1 h, the relative amount of stereocomplex crystallization attains 36%, reaching complete stereocomplexation after 24 h. These data indicate that the homocrystals of polylactide, after remelting at 190°C, can recrystallize selectively as stereocomplex during annealing.[10]

Figure 3 shows the DSC curves for the 50/50 blend annealed for 24 h at the temperatures listed in Table III. Curves "a" and "b" correspond to samples annealed for 24 h at 140 and 160°C, where the formation of the homocrystal is favored against stereocomplexation as explained previously, and show therefore intense endotherms. However, the endothermic peak centered around 170°C, that appears in curves "c" (sample annealed at 180°C) and "d" (after annealing at 190°C) corresponds to the small fraction of homocrystals formed during the cooling step after the annealing treatment, as a result of incomplete stereocomplex crystallization. Notice that at these annealing temperatures the homocrystal is melted and does not crystallize. Since the cooling step covers the whole range of crystallization temperatures, these crystals may be a mixture of crystals of different perfections, but they are homocrystals in any case.

As can be seen, double melting peaks appear with increasing annealing temperature as a consequence of the structural reorganization of the chains. The crystals corresponding to the intermediate peaks between those of the homocrystal and the high melting stereocomplex act as precursors for the formation of the final stereocomplex. The occurrence of double melting endotherms during DSC heating of polymers has been reported for several semicrystalline polymers.[54–59] Two models have been proposed to explain this phenomenon, the double lamellar thickness model[60,61] and the melting of the thinner lamellae.[62,63] The double lamellar thickness model is associated with the existence of two populations of crystalline lamellae with different thicknesses. The melting of the thinner lamellae gives rise to the low endotherms and melting of the thicker lamellae to the high endotherm. The melting recrystallization model postulates that the low temperature endotherm arises from melting of most of the lamellae initially present. The partially melted amorphous material then undergoes a continuous

Table III. Thermal Properties Measured by DSC of Polylactide Equimolar Blends at Different Crystallization Temperatures and Times

	1 h				24 h			
Annealing T (°C)	ΔH_H (J/g)	ΔH_S (J/g)	X_{stereo} (%)	X_c (%)	ΔH_H (J/g)	ΔH_S (J/g)	X_{stereo} (%)	X_c (%)
140	36.3	8.1	18	39	59.3	9.2	13	62
160	46.8	8.1	15	49	60.5	11.7	16	65
180	47.5	9.4	16	33	6.4	56.9	90	41
190	30.4	17.0	36	18	-	85.2	100	60

Melting enthalpy of homocrystals (ΔH_H), stereocomplex crystals (ΔH_S), stereocomplex fraction of the total crystallinity (X_{stereo}), and overall crystallinity (X_c).[10]

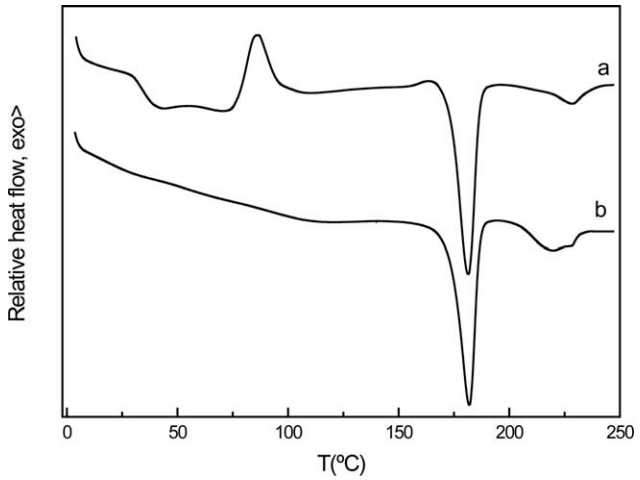

Figure 4. DSC thermograms of 50/50 blends of high molecular weight polylactides (a) without MWCNTs and (b) with 1.5 wt % of MWCNTs.

process of recrystallization into thicker, more perfect lamellae, which melt at higher temperatures.[64]

Effect of MWCNTs on the Stereocomplexation of PDLA/PLLA Blends

This study investigates the addition of MWCNTs to PDLA/PLLA blends with the aim of analyzing the crystallization behavior and the nucleation efficiency of the MWCNTs in the polylactide stereocomplex crystals, since their effectiveness as nucleating agents has been shown in several polymeric matrices.[65–67]

Figure 4 displays the DSC thermograms of 50/50 blends containing 0 and 1.5 wt % of MWCNTs. As can be seen, the addition of small amounts of MWCNTs to the blend removes the recrystallization peak, also termed cold crystallization, associated with the formation of crystals during heating. This result indicates that MWCNTs favor the crystallization of PLLA, in addition the overall crystallinity increases from 13.5% for the sample without MWCNTs to 28.8% for the nanocomposite containing 1.5 wt % of MWCNTs. In consequence, the addition of MWCNTs improves the crystallization of the polylactide matrix.

Figure 5 shows the evolution of the melting enthalpy of the homocrystal and the stereocomplex, along with the overall crystallinity degree, with the content of MWCNTs during the first DSC scan for the solvent cast 50/50 blends. As can be seen, the addition of MWCNTs increases the melting enthalpy of the stereocomplex while the one of the homocrystal decreases, showing reduced values for nanocomposites containing 3.0 wt % of MWCNTs. On the other hand, the overall crystallinity degree increases upon the addition of small amounts of MWCNTs, but decreases again for nanotube contents above about 0.5 wt %.

As discussed before, during a heating DSC scan only a limited extent of stereocomplexation can be usually achieved in high molecular polylactide enantiomeric blends, hence, appropriate thermal treatments were carried out to achieve full stereocomplexation now in presence of MWCNTs. For the nanocomposite containing 1.0 wt % of MWCNTs in the equimolar blend, annealing at 180°C for 4 h was found enough to achieve full stereocomplexation. Hence, the addition of MWCNTs allows achieving full stereocomplexation with milder thermal treatments, since the annealing temperature and time are reduced from 190°C to 180°C, and from 24 h to about 4 h respectively. The melting enthalpy with MWCNTs is, however, smaller (34 J/g) than without the nanotubes (85 J/g). This decrease in melting enthalpy of stereocomplex together with the decreasing of overall crystallinity by adding larger amounts of MWCNTs may be due to the formation of agglomerates as a consequence of the poor dispersion of the MWCNTs in the matrix.

Effect of Pyrene Terminal Group in the Stereocomplexation of PDLA/PLLA Blends

In this study, py-end-PLLA was used with the aim of getting two different enhancing effects. On the one hand, it is expected to improve the dispersion of MWCNTs due to the presence of pyrene terminal group that interact with MWCNTs, while on the other hand, 50/50 blends of py-end-PLLA and PDLA were carried out to verify that end-functionalized PLLA short chains interact with the PDLA matrix to favor stereocomplex crystals formation.

Figure 6 shows TEM images of the nanocomposites containing 1.0 wt % MWCNTs. In Figure 6(A), the polymer matrix is PLLA ($M_n = 24900$, Table II), and the TEM image shows large aggregates (of about 270 μm) suggesting a poor dispersion of the nanotubes. In Figure 6(B), the polymer matrix is py-end-PLLA of the same molecular weight (Table II), and the TEM image reveals individual MWCNTs randomly dispersed, as a consequence of the presence of the terminal pyrene groups, confirming a fine and homogeneous dispersion in the matrix.

Changing the molecular weight of the py-end-PLLA chains can affect the nanocomposites in several ways. On the one hand, lower molecular weights imply a larger amount of pyrene end-groups per nanotube (for a given MWCNT composition), and may favor the dispersion of the nanoreinforcing particles. On the other hand, lower molecular weights favor preferentially the formation of stereocomplex crystals instead of homopolymer

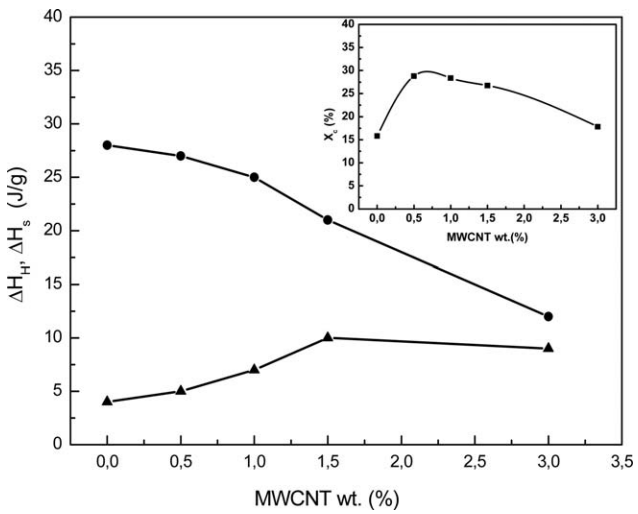

Figure 5. Evolution of melting enthalpy of (●) homocrystals (ΔH_H), (▲) stereocomplex crystals (ΔH_H), and (■) overall crystallinity (X_c) with the content of MWCNTs in 50/50 blends prepared as cast.

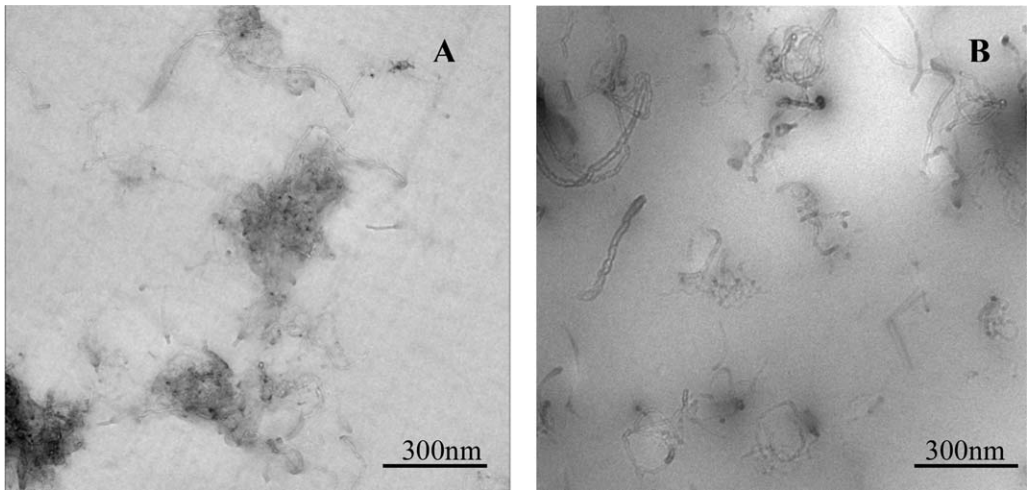

Figure 6. TEM images of (A) PLLA/MWCNTs and (B) PLLA/py-end-PLLA/MWCNTs.

crystallites according to previously published results.[3] To analyze these effects, equimolar PDLA/py-end-PLLA mixtures were prepared using py-end-PLLA chains with three different molecular weights (2900, 9000, and 24,900 g/mol, Table II).

Figure 7 graphs the first DSC scans for as cast py-end-PLLA/PDLA blends prepared using py-end-PLLA chains of different molecular weights. As can be seen, when low molecular weight py-end-PLLA (2900 or 9000 g/mol) is blended with PDLA, similar traces can be observed. In both cases, full stereocomplexation occurs spontaneously during casting, producing in the DSC analyses significant endothermic peaks of 38 and 43 J/g, at temperatures about 209°C, due to stereocomplex crystal melting. These results indicate easy stereocomplexation with low molecular weights. In contrast, the PDLA/py-end-PLLA24900 matrix shows a completely different behavior, since this system shows three endothermic peaks at about 142, 175, and 209°C, corresponding to py-end-PLLA homocrystallites (as shown in Table II), PDLA homocrystallites and stereocomplex crystallites, respectively. In addition, an exothermal peak with $\Delta H_c \approx 16$ J/g is observed at about 83°C. This enthalpy value corresponds approximately to the sum of the three melting enthalpies observed; hence, crystallization is concluded to occur during the heating scan.

Numerous methods have been reported for tracing polylactide stereocomplexation, particularly X-ray diffraction studies have been often used to separate homocrystallization and stereocomplexation in polylactides.[68] Another alternative is FTIR spectroscopy, since the C=O stretching band of the stereocomplex is red shifted relative to the homocrystals (the former is located at about 1748 cm^{-1} and the latter at about 1759 cm^{-1}) due mainly to C–H···O=C hydrogen bonding interactions.[10] In addition, ^{13}C NMR spectroscopy can be also an effective method for detecting polylactide stereocomplexation.[2] This technique has been used in this work to gain insight on the microstructure of the nanocomposites investigated in this article.

Figure 8 shows the ^{13}C NMR spectrum of the carbonyl carbon of as cast PDLA, py-end-PLLA and their equimolar blends. Pristine PDLA [Figure 8(a)] shows a broad peak in which the

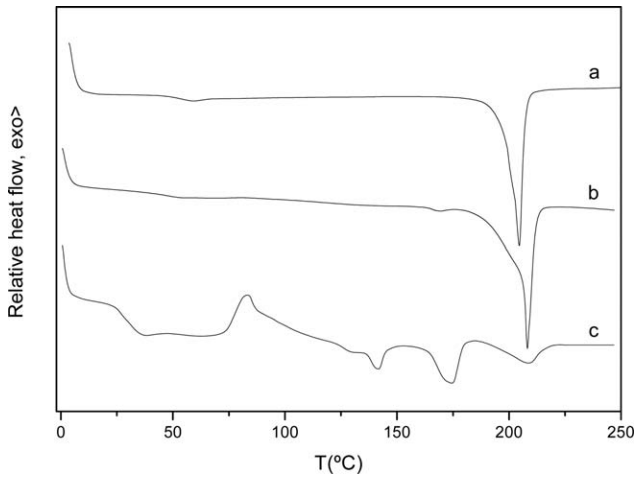

Figure 7. DSC curves of PDLA/py-end-PLLA blends with py-end-PLLA chains of (a) 2900 g/mol, (b) 9000 g/mol, and (c) 24,900 g/mol.

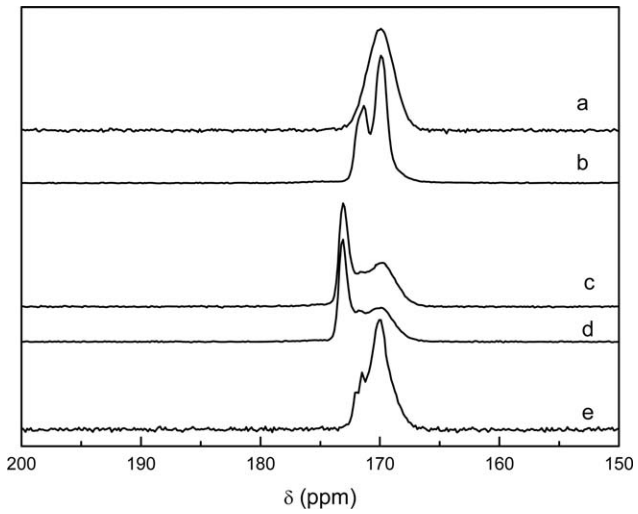

Figure 8. 1D 13C_NMR spectra of carbonyl carbon region in (a) PDLA, (b) py-end-PLLA9000, (c) PDLA/py-end-PLLA2900, (d) PDLA/py-end-PLLA9000, and (e) PDLA/py-end-PLLA24900.

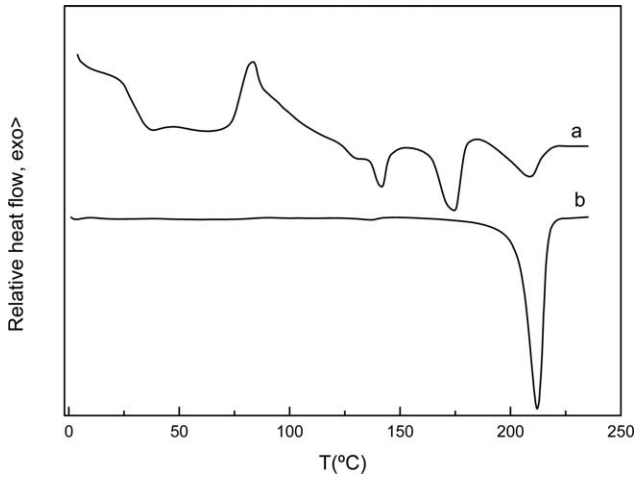

Figure 9. DSC curves of equimolar (a) PDLA/py-end-PLLA24900 and (b) PDLA/PLLA24900 blends.

maximum contribution corresponds to the amorphous phase at 170 ppm, while pure py-end-PLLA [Figure 8(b)] shows resolved amorphous and homocrystal peaks at 170 and 172 ppm, respectively. These values are in agreement with those obtained by other authors for polylactides.[2] The different behavior between both enantiomers can be assigned to the different molecular weights. The equimolar blends of PDLA with the py-end-PLLA samples of lower molecular weight, spectra 8(c) and 8(d), show a new peak at 173.1 ppm corresponding to the carbonyl carbon in the stereocomplex crystals. However, in the equimolar blend of PDLA with py-end-PLLA24900, the main contribution indicates again that the polymer matrix is mainly in the amorphous state, and the small shoulders indicate the presence of minor amounts of homocrystals. In conclusion, NMR results agree with those obtained by DSC, indicating that the py-end-PLLA of higher molecular weight does not crystallize during the casting step.

To evaluate the effect of the pyrene end-group on the crystallization process, PDLA has been blended with PLLA24900 with and without functional end-groups. Figure 9 shows the first DSC scans for the as cast PDLA/py-end-PLLA24900 [Figure 9(a)], and the PDLA/PLLA24900 systems [the latter lacking end-pyrene groups, Figure 9(b)]. As can be seen, the PDLA/PLLA24900 blend crystallizes completely in the stereocomplex form while the system modified with pyrene is amorphous as previously observed. The results suggest that the presence of pyrene in PDLA/py-end-PLLA24900 blends hinders the stereocomplexation.

With the purpose of corroborating this hypothesis, the transport properties of py-end-PLLA and PLLA molecules were determined by the Diffusion ordered NMR spectroscopy (DOSY) method.[69] DOSY experiments of py-end-PLLA24900 and PLLA24900 using chloroform as solvent were carried out as shown in Figure 10. PLLA24900 has an average log *D* value of 8.03, whiles the same DOSY experiment for py-end-PLLA24900 shows a value of 8.52. The difference between the two diffusion coefficients is quite significant; indicating that in spite of the same size of the PLLA chains, the diffusion of PLLA is faster than that of py-end-PLLA. This indicates that the pyrene group prevents the mobility of the PLLA chain; due to the existence of many pyrene groups interacting between them by $\pi-\pi$ interactions. Similar $\pi-\pi$ anchoring systems can be found in literature for pyrene derivates in which π conjugated molecules are used for chiral organization[70] and for fullerene-end groups, showing self-assembly of fullerenes that results in nanoscale aggregates.[71]

To summarize, when the pyrene group is end-functionalized to the shorter PLLA chains (2900 and 9000 g/mol), the PLLA chains can move more easily and reach a PDLA segment to crystallize as stereocomplex, in agreement with the conclusions drawn from the DSC analysis. However, when py-end-PLLA24900 (the py-end-PLLA with the highest molecular weight) is used, the stereocomplex crystallization is prevented due to the $\pi-\pi$ stacking of aromatic rings. These interactions are so strong that pyrene-pyrene groups form aggregates decreasing the mobility of the PLLA chains in the blend and hindering the approximation of the enantiomeric molecules, required for the formation of the stereocomplex crystals (Figure 11).

Effect of MWCNTs in the Stereocomplexation of PDLA/py-end-PLLA Blends

The addition of MWCNTs should favor the crystallization of the PDLA/py-end-PLLA24900 blends, and might compensate the adverse effect attributed to the pyrene end-groups. Figure 12(i) presents the thermal behavior of the PDLA/py-end-PLLA24900 blends with 1.0 wt % MWCNTs and without MWCNTs. In the first DSC scan, both samples show three different melting peaks at about 140, 175, and 210°C, corresponding to py-end-PLLA homocrystals, PLLA homocrystals and stereocomplex crystals, respectively. However, the blend without MWCNTs crystallizes during the heating scan, indicating an initially amorphous sample, while the system with 1.0 wt % MWCNTs does not show any crystallization during heating, suggesting that the as cast sample was already crystallized. The Figure 12(ii) shows the X-ray diffraction profiles for samples previously analyzed by DSC. Figure 12(i-a) shows no characteristic diffraction peaks of any type of crystal. Therefore, it may be concluded that the

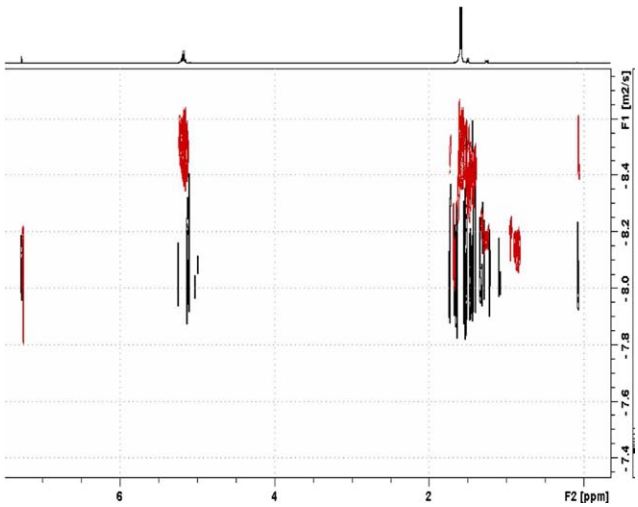

Figure 10. DOSY spectra of py-end-PLLA24900 (in red color) and PLLA24900 (in black color). [Color figure can be viewed in the online issue, which is available at wileyonlinelibrary.com.]

Applied Polymer SCIENCE

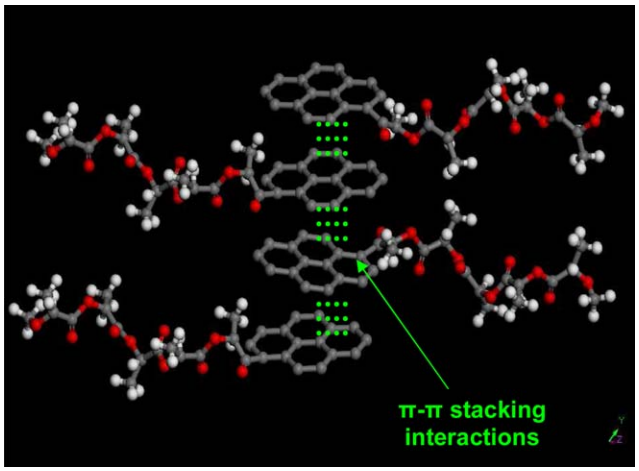

Figure 11. Pyrene end-group agglomerations in PDLA/py-end-PLLA24900 system in absence of MWCNTs (carbon atoms in grey, oxygens in red, and hydrogens in black). [Color figure can be viewed in the online issue, which is available at wileyonlinelibrary.com.]

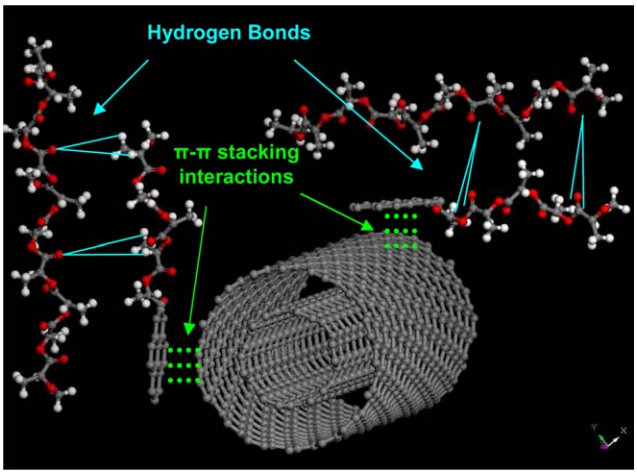

Figure 13. Interactions between MWCNTs and pyrene groups of pyrene-end-PLLA chains in PDLA/py-end-PLLA/MWCNTs (carbon atoms in grey, oxygens in red, and hydrogens in black). [Color figure can be viewed in the online issue, which is available at wileyonlinelibrary.com.]

sample is totally amorphous at room temperature. However, the curve 12(i-c) for the nanocomposite with 1.0 wt % MWCNTs shows the diffractions due to stereocomplex crystals ($2\theta = 12$, 21, and 24°) and those of homocrystals ($2\theta = 14.5$, 16.5, and 18.7°). These data support the DSC results.

The upper insert in Figure 12(i) shows the cooling traces, and as can be seen the blend with 1.0 wt % of MWCNTs crystallizes at 111°C with an enthalpy value of 22 J/g, while the blend without MWCNTs crystallizes at 101°C with an enthalpy value of 3 J/g. Concerning to the second run, the sample without MWCNTs shows two melting peaks, one corresponding to the stereocomplex formed during cooling and another one to the homocrystal formed during heating in the second run. However, the blend with 1.0 wt % MWCNTs shows a single melting peak at about 190°C, which can be attributed to the stereocomplex crystals as Figure 12(ii-d) shows.

These results indicate that MWCNTs can act as an effective nucleating agent, specifically favoring the formation of the stereocomplex. The favorable effect of the MWCNTs is probably enhanced by the fact that the unfavorable pyrene–pyrene π–π

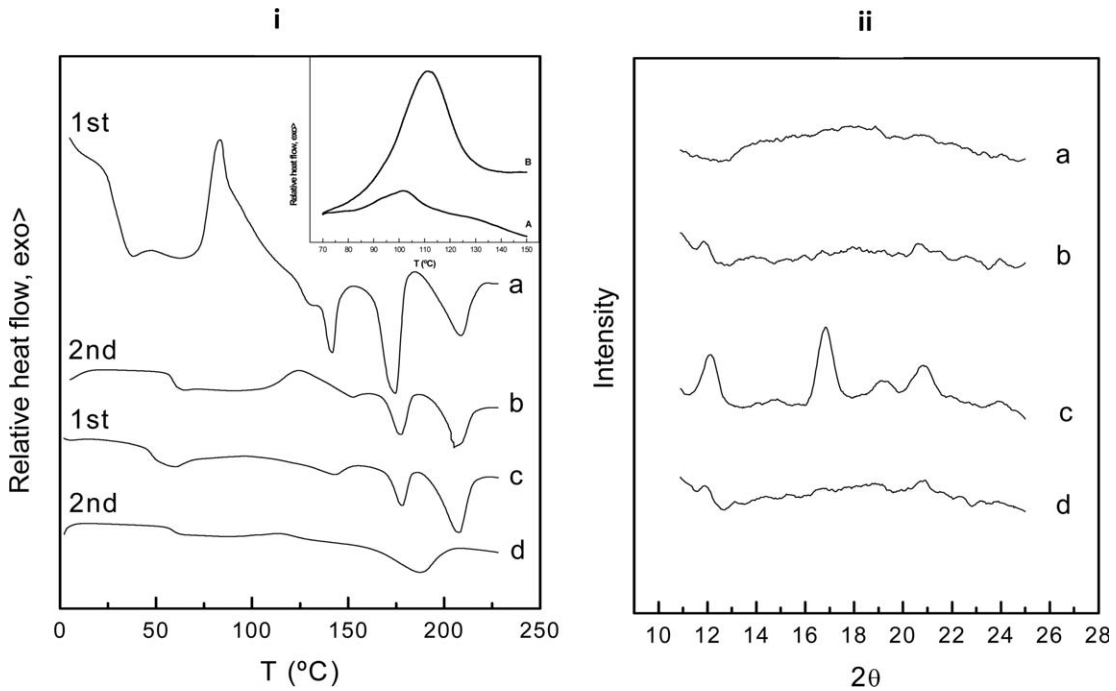

Figure 12. (i) DSC curves of first and second runs, and (ii) X-ray diffraction patterns corresponding to PDLA/pyPLLA24900 (a,b) without MWCNTs and (c,d) with 1.0 wt % of MWCNTs. The cooling scan at 5°C/min is shown in the upper side square being the blend (A) without MWCNTs and (B) with 1.0 wt % of MWCNTs.

Table IV. Annealing of PDLA/py-end-PLLA24900 with 1.0 wt % of MWCNTs and Without MWCNTs for 1 h at Different Crystallization Temperatures

MWCNT wt %	0%				1%			
Annealing	ΔH_H (J/g)	T_{mH} (°C)	ΔH_S (J/g)	T_{mS} (°C)	ΔH_H (J/g)	T_{mH} (°C)	ΔH_S (J/g)	T_{mS} (°C)
As-cast	8.4	178.6	4.90	210.0	4.9	175.0	9.6	209.0
1 h-120°C	16.7	173.6	15.2	206.7	-	-	46.1	198.8
1 h-140°C	36.3	174.2	8.1	206.9	5.6	172.1	34.8	205.7
1 h-160°C	46.8	174.4	8.1	207.2	-	-	48.4	207.3

interactions should be counterbalanced by the favorable pyrene–MWCNT π–π interactions (Figure 13). Thus, the addition of MWCNTs should prevent the formation of aggregates, promoting the homogeneous dispersion of the chains, and therefore the stereocomplexation.

However, to achieve full stereocomplexation and high perfection crystals, specific thermal treatments are still required. Table IV shows the DSC results obtained with the equimolar PDLA/py-end-PLLA24900 blends containing 0 and 1.0 wt % MWCNTs annealed at temperatures up to 160°C. On the one hand, when the 50/50 blend without MWCNTs is annealed for 1 h at different temperatures, homocrystal formation prevails over stereocomplex crystallization. Increasing the selected crystallization temperature increases the amount of homocrystallization, while the amount of stereocomplex crystals remains nearly unchanged. However, this behavior is radically changed upon the addition of MWCNTs, since stereocomplex formation is favored against homocrystallization. When the blend is annealed at 120°C for 1 h, the melting of the stereocomplex crystals occurs at about 200°C. Annealing at 140°C for 1 h improves the perfection of the stereocomplex crystals, increasing the melting temperature to about 206°C, but a small amount of homocrystal is also present, hence, incomplete stereocomplexation occurs. However, annealing at 160°C for 1 h was found enough to achieve full stereocomplexation, obtaining high perfection stereocomplex crystals with a melting temperature at about 210°C. These findings prove that the addition of MWCNTs improves the selective formation of stereocomplex especially with the aid of specific thermal treatments.

CONCLUSIONS

This article investigates different strategies to improve the formation of polylactide stereocomplex crystals. Initially, equimolar blends of PLLA and PDLA of high molecular weight were studied. The main crystalline formation in these blends was homocrystal, and a harsh annealing at 190°C for 24 h was found necessary to achieve complete stereocomplexation. The addition of low contents of MWCNTs to 50/50 blends was found to enhance the overall crystallinity and the stereocomplex crystallization since full stereocomplexation was achieved with less aggressive annealing, at 180°C for 4 h. However, a poor dispersion of MWCNTs leads to the formation of agglomerates restricting the stereocomplex crystallization.

When py-end-PLLA of 2900 and 9000 g/mol were blended with PDLA, full stereocomplexation was obtained in the as cast blends, whereas in PDLA/py-end-PLLA24900 blends DOSY experiments indicated that the pyrene end-group prevented the arrangement of L- and D-units required to obtain the stereocomplex crystals due to the agglomeration of pyrene-end-groups by $\pi-\pi$ stacking interactions.

The addition of MWCNTs to the PDLA/py-end-PLLA24900 system promoted the spontaneous crystallization of the nanocomposite, and slightly enhanced the selective stereocomplex crystallization. This behavior is attributed to the occurrence of pyrene–MWCNT π–π interactions that compete with the formation of agglomerates through pyrene–pyrene π–π stacking interactions. The pyrene–MWCNTs coupling favors the mobility of the PLLA chains (end-functionalized by pyrene groups), allowing the formation of hydrogen bonds with the PDLA matrix and in consequence, the full stereocomplexation is achieved in even milder annealing conditions of 1 h at 160°C.

ACKNOWLEDGMENTS

Authors are thankful for funds of the European Union project POCO (7th Framework Program NMP-213939). Basque Government, Department of Education, Linguistic Politics and Culture (GIC12/161-IT-632-13), Department of Industry (IE 10/276) and University of the Basque Country (UFI11/55) are also thanked. I. Martínez de Arenaza and N. López are post-doctoral fellows of the University of the Basque Country. SGIker (UPV/EHU) technical support for WAXD, TEM and NMR measurements is also gratefully acknowledged. Authors also would also like to thank the 7th F. P. of E.U. project F.R.S.-FNRS for financial support. CIRMAP is very grateful to "Région Wallonne" and European Union (FEDER, FSE) for general financial support in the frame of Objectif 1-Hainaut: Materia Nova, as well as to the Belgian Federal Government Office of Science Policy (SSTC-PAI 6/27). J-M. Raquez is "Chargé de recherche" by the Belgian F.R.S-FNRS.

REFERENCES

1. Gupta, A.P.; Kumar, V. *Eur. Polym. J.* **2007**, *43*, 4053.
2. Tsuji, H. *Macromol. Biosci.* **2005**, *5*, 569.
3. Ikada, Y.; Jamshidi, K.; Tsuji, H.; Hyon, S.H. *Macromolecules* **1987**, *20*, 904.
4. Rahman, N.; Kawai, T.; Matsuba, G.; Nishida, K.; Kanaya, T.; Watanabe, H.; Okamoto, H.; Kato, M.; Usuki, A.;

Matsuda, M.; Nakajima, K.; Honna, N. *Macromolecules* **2009**, *42*, 4739.

5. Miyata, T.; Masuko, T. *Polymer* **1998**, *39*, 5515.
6. Spinu, M.; Jackson, C.; Keating, M.Y.; Gardner, K.H. *J. Macromol. Sci. Pure. Appl. Chem.* **1996**, *A33*, 1497.
7. Fukushima, K.; Furuhashi, Y.; Sogo, K.; Miura, S.; Kimura, Y. *Macromol. Biosci.* **2005**, *5*, 21.
8. Loomis, G.L.; Murdoch, J.R.; Gardner, K.H. *Polym. Prep.* **1990**, *31*, 55.
9. Tsuji, H.; Ikada, Y. *Macromolecules* **1992**, *25*, 5719.
10. Sarasua, J.R.; López Rodríguez, N.; López Arraiza, A.; Meaurio E. *Macromolecules* **2005**, *38*, 8362.
11. Xu, H.; Teng, C.; Muhuo, Y. *Polymer* **2006**, *47*, 3922.
12. Anderson, K.S.; Hillmyer, M.A. *Polymer* **2006**, *47*, 2030.
13. Tsuji, H.; Ikada, Y. *Polymer* **1999**, *40*, 6699.
14. Tsuji, H. *Polymer* **2000**, *41*, 3621.
15. Tsuji, H. *Biomaterials* **2003**, *24*, 537.
16. Sarasua, J.R.; Lopez Arraiza, A.; Balerdi, P.; Maiza, I. *J. Mater. Sci.* **2005**, *40*, 1855.
17. Sarasua, J.R.; Prud'homme, R.E.; Wisniewski, M.; Le Borgne, A.; Spassky, N. *Macromolecules* **1998**, *31*, 3895.
18. Tsuji, H.; Nakano, M.; Hashimoto, M.; Takashima, K.; Katsura, S.; Mizuno, A. *Biomacromolecules* **2006**, *7*, 3316.
19. Masaki, D.; Fukuy, Y.; Toyohara, K.; Ikegame, M.; Nagasaka, B.; Yamane, H. *Sen'i Gakkaishi* **2008**, *64*, 212.
20. Xu, C.; Qiu, Z. *J. Polym. Sci. Part B: Polym. Phys.* **2009**, *47*, 2238.
21. Liu, T.; Phang, I.; Shen, L.; Chow, S.; Zhang, W. *Macromolecules* **2004**, *37*, 7214.
22. Li, X.; Huang, Y.; Liu, L.; Cao, H. *J. Appl. Polym. Sci.* **2006**, *102*, 2500.
23. Baughman, R.H.; Zakhidov, A.A.; de Heer, W.A. *Science* **2002**, *297*, 787.
24. Berber, S.; Kwon, Y.; Tomanek, D. *Phys. Rev. Lett.* **2000**, *84*, 4613.
25. Tans, S.; Devoret, M.; Dai, H.; Thess, A.; Smalley, R.; Geerlings, L.; Dekker, C. *Nature* **1997**, *386*, 474.
26. Meuer, S.; Braun, L.; Schilling, T.; Zentel, R. *Polymer* **2009**, *50*, 154.
27. Chen, S.; Wu, G.; Liu, Y.; Long, D. *Macromolecules* **2006**, *39*, 330.
28. Srebnik, S. *J. Polym. Sci. Part B: Polym. Phys.* **2008**, *46*, 2711.
29. Yuan, W.Z.; Mao, Y.; Zhao, H.; Sun, J.Z.; Xu, P.H.; Jin, J.K.; Zheng, Q.; Tang, B.Z. *Macromolecules* **2008**, *41*, 701.
30. Sun, Y.P.; Fu, K.; Lin, Y.; Huang, W. *Acc. Chem. Res.* **2002**, *35*, 1096.
31. Tasis, D.; Tagmatarchis, N.; Georgakilas, V.; Prato, J.M. *Chem. Eur.* **2003**, *9*, 4000.
32. Szleifer, I.; Yerushalmi-Rozen, R. *Polymer* **2005**, *46*, 7803.
33. Rouse, J.H. *Langmuir* **2005**, *21*, 1055.
34. Nativ-Roth, E.; Shvartzman-Cohen, R.; Bounioux, C.; Florent, M.; Zhang, D.; Szleifer, I. *Macromolecules* **2007**, *40*, 3676.
35. Chen, R.J.; Zhang, Y.; Wang, D.; Dai, H. *J. Am. Chem. Soc.* **2001**, *123*, 3838.
36. Meyer, F.; Raquez, J.M.; Coulembier, O.; De Winter, J.; Gerbaux, P.; Dubois, P. *Chem. Commun.* **2010**, *46*, 5527.
37. Meyer, F.; Minoia, A.; Raquez, J.M.; Spasova, M.; Lazzaroni, R.; Dubois, P. *J. Mater. Chem.* **2010**, *20*, 6873.
38. Meuer, S.; Braun, L.; Zentel, R. *Macromol. Chem. Phys.* **2009**, *210*, 1528.
39. Yang, Q.; Shuai, L.; Zhou, J.; Lu, F.; Pan, X. *J. Phys. Chem. Part B* **2008**, *112*, 12934.
40. Choi, I.H.; Park, M.; Lee, S.S.; Hong, S.H. *Eur. Polym. J.* **2008**, *44*, 3087.
41. Yang, Q.; Shuai, L.; Zhou, J.; Lu, F.; Pan, X. *J. Phys. Chem. Part B* **2008**, *112*, 12934.
42. Petrov, P.; Stassin, F.; Pagnoulle, C.; Jérôme, R. *Chem. Commun.* **2003**, 2904.
43. Lou, X.; Daussin, D.; Cuenot, S.; Duwez, A.S.; Pagnoulle, C.; Detrembleur, C.; Bailly, C.; Jerome, R. *Chem. Mater.* **2004**, *16*, 4005.
44. Zhao, X.; Ye, L. *Compos. Part B* **2011**, *42*, 926.
45. Schmidt, S.C.; Hillmyer, M.A. *J. Polym. Sci. Part B: Polym. Phys.* **2001**, *49*, 3000.
46. Kolstad, J.J. *J. Appl. Polym. Sci.* **1996**, *62*, 1079.
47. Ray, S.S.; Yamada, K.; Okamoto, M.; Ogami, A.; Ueda, K. *Chem. Mater.* **2003**, *15*, 1456.
48. Li, J.; Chen, D.; Gui, B.; Gu, M. *J. Ren. Polym. Bull.* **2011**, *67*, 775.
49. Nam, J.Y.; Okamoto, M.; Okamoto, H.; Nakano, M.; Usuki, A.; Matsuda, M. *Polymer* **2006**, *47*, 1340.
50. Kawamoto, N.; Sakai, A.; Horikoshi, T.; Tobita, E. *J. Appl. Polym. Sci.* **2007**, *103*, 198.
51. Kawamoto, N.; Sakai, A.; Horikoshi, T.; Urushihara, T.; Tobita, E. *J. Appl. Polym. Sci.* **2007**, *103*, 244.
52. Schmidt, S.C.; Hillmyer, M.A. *J. Polym. Sci. Part B: Polym. Phys.* **2001**, *39*, 300.
53. Yamane, H.; Sasai, K. *Polymer* **2003**, *44*, 2569.
54. Sauer, B.B.; Kampert, W.G.; Blanchard, E.M.; Threefoot, A.S.; Hsiao, B.S. *Polymer* **2000**, *41*, 1099.
55. Wei, C.L.; Chen, M.; Yu, F.E. *Polymer* **2003**, *44*, 8185.
56. Tan, S.; Su, A.; Li, W.; Zhou, E. *J. Polym. Sci. Part B: Polym. Phys.* **2000**, *38*, 53.
57. Yasuniwa, M.; Satou, T. *J. Polym. Sci. Part B: Polym. Phys.* **2002**, *40*, 2411.
58. Qiu, Z.; Komura, M.; Ikehara, T.; Nishi, T. *Polymer* **2003**, *44*, 7781.
59. Gunaratne, L. M. W. K.; Shanks, R.A. *J. Polym. Sci. Part B: Polym. Phys.* **2006**, *44*, 70.
60. Cebe, P.; Hong, S.D. *Polymer* **1986**, *27*, 1183.
61. Bassett, D.C.; Olley, R.H.; Raheil, I. A. M. *Polymer* **1988**, *29*, 1745.

62. Lee, Y.; Porter, R.S.; Lin, J.S. *Macromolecules* **1989**, *22*, 1756.
63. Jonas, A.M.; Russell, T.P.; Yoon, D.Y. *Macromolecules* **1995**, *28*, 8491.
64. Shieh, Y.T.; Liu, G.L. *J. Polym. Sci. Part B: Polym. Phys.* **2007**, *45*, 1870.
65. Zhu, Y.; Du, Z.; Li, H.; Zhang, C. *Polym. Eng. Sci.* **2011**, *51*, 1770.
66. Yu, J.; Grobner, G.; Tonpheng, B.; Anderson, O. *Polymer* **2011**, *52*, 5521.
67. Panda, B.; Bhattacharyya, A.R.; Kulkarni, A.R. *Polym. Eng. Sci.* **2011**, *5*, 1550.
68. Brizzolara, D.; Cantow, H-J.; Diederichs, K.; Keller, E.; Domb, A. *J. Macromolecules* **1996**, *29*,191.
69. Johnson, C.S., Jr. *Prog. Nucl. Magn. Reson. Spectrsc.* **1999**, *34*, 203.
70. Sperling, L.H. Introduction to Physics Polymer Science, 4th ed.; Wiley: Hoboken, NJ, **1992**.
71. Hoffman, J.D. *Polymer* **1983**, *24*, 3.